Supporting Information

Modulating Electrons Population Pathways for Time-dependent Dynamic Multicolor Display

Weixin Xu, Lei Lei,* Yubin Wang, Enyang Liu, Liang Chen, Shiqing Xu*

Institute of Optoelectronic Materials and Devices, College of Optical and Electronic Technology, China Jiliang University, Hangzhou 310018, China

Experimental Section

Materials: All the raw chemicals were of analytical grade and were directly used as received without further refinement. Oleic acid (OA) was offered by Sigma Aldrich Company. Ammonium fluoride (NH_4F), erbium nitrate pentahydrate ($Er(NO_3)_3·5H_2O$), thulium nitrate hexahydrate ($Tm(NO_3)_3·6H_2O$), holmium nitrate pentahydrate ($Ho(NO_3)_3·5H_2O$), ytterbium nitrate pentahydrate ($Yb(NO_3)_3·5H_2O$) and Hafnium (IV) acetylacetonate were all supplied by Aladdin Chemical Reagent Company. Sodium oleate (NaOA) and Oleylamine (OM) were bought from Macklin Chemical Reagent Company. The cyclohexane and ethanol were purchased from Sinopharm Chemical Reagent Company. Deionized water was used throughout.

Synthesis of lanthanide-doped Na_3HfF_7 NCs: In a typical procedure, taking Er^{3+}: Na_3HfF_7 as an example, Hafnium (IV) acetylacetonate (1mmol*x%), $Er(NO_3)_3·5H_2O$ (1mmol*(1-x%)) and 20mL ethanol were added into a 50 mL beaker and stirred for 10 min. Then 12mL OA, 2.5mL OM and 2.5g NaOA were added into the above mixture with continuous stirring for another 20 min followed by the addition of 5mL deionized water containing 10 mmol NH_4F. After stirring at room temperature for about 30 min, the above solution was transferred into a 40 mL Teflon-lined autoclave, sealed and heated at 130 ^oC for 12 h. After the solution cooled down to room temperature, the product were precipitated via the addition of ethanol, collected via centrifugation at 11000 rpm for 5 min, washed three times with ethanol/cyclohexane, and finally the product was dispersed in 4 mL cyclohexane solution for further usage.

Characterizations: The X-ray diffraction (XRD) analysis was carried out with a

powder diffractometer (Bruker D8 Advance) using Cu-K_α (λ=1.5405 Å) radiation. The shape of the samples and size of the as-prepared products were characterized by a scanning electron microscopy (SEM). High resolution image of the products were characterized by a field emission transmission electron microscopy (TEM, FEI Tecnai G2 F20) equipped with an energy dispersive X-ray spectroscope (EDX, Aztec X-Max 80T). TEM specimens were prepared by drying a drop of a dilute cyclohexane dispersion solution of the products on the surface of a carbon-coated copper grid. Upconversion emission spectra were carried out on an Edinburgh Instruments FLS920 spectrofluorimeter upon 980 nm excitation by a power-controllable 980 nm diode laser. Scintillation spectra were recorded on an OmniFluo-Xray-JL system (PMT-CR131-TE detector, 185-900 nm) with a mini MAGPRO X-ray excitation source. All photoluminescence studies were carried out at room temperature.

Figure S1-S13

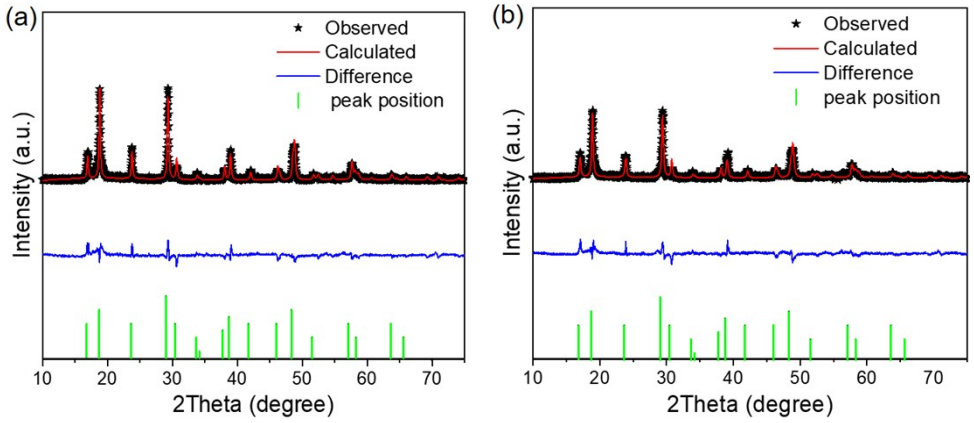

Figure S1. Rietveld refinement XRD patterns of the pure Na_3HfF_7 (a) and Na_3HfF_7: 2Yb/6Er NPs (b).

As shown in Figure S1a, the observed and calculated diffraction patterns for the Na_3HfF_7 host were in accordance well with each other, revealing the host exhibited pure hexagonal phase. The values of Rp and Rwp were 6.52% and 7.95%, respectively. Similar results were achieved for the Na_3HfF_7: 2Yb/6Er NPs as well (Figure S1b). In comparison with the pure Na_3HfF_7 host (a=b=5.3061 Å, c=10.4968 Å), the Na_3HfF_7: 2Yb/6Er NPs exhibited relatively smaller lattice parameters of a=b=5.2957 Å and

c=10.4883 Å. Considering the ionic radius of Yb^{3+} (0.112 nm) and Er^{3+} (0.114 nm) ions are larger than that of Hf^{4+} (0.097 nm) ions, the substitution of Hf^{4+} ions by Yb/Er codopants should lead to the expansion of the crystal lattice. Thus, the lattice contraction revealed by the Rietveld XRD refinement further suggesting the formation of vacancies in the crystal structure after incorporating Yb/Er codopants.

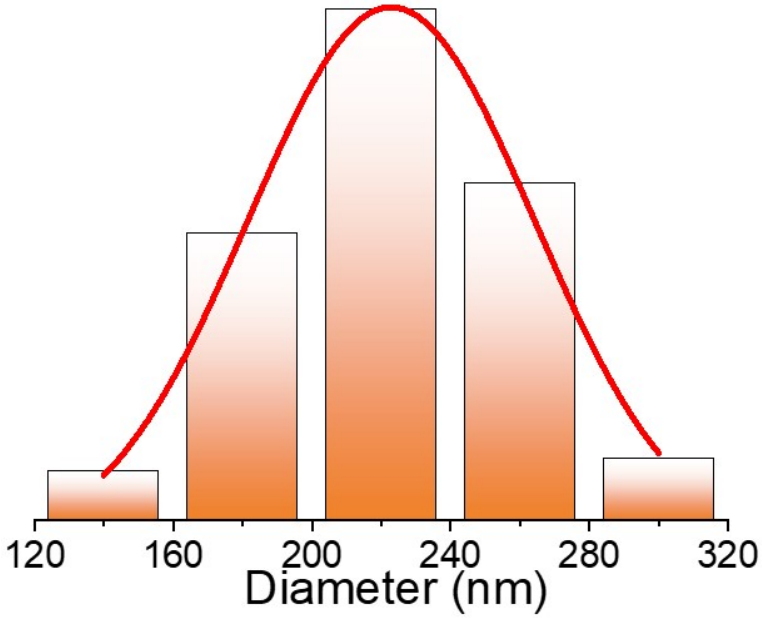

Figure S2. Histogram size distribution of the Na_3HfF_7: 2Yb/6Er NPs.

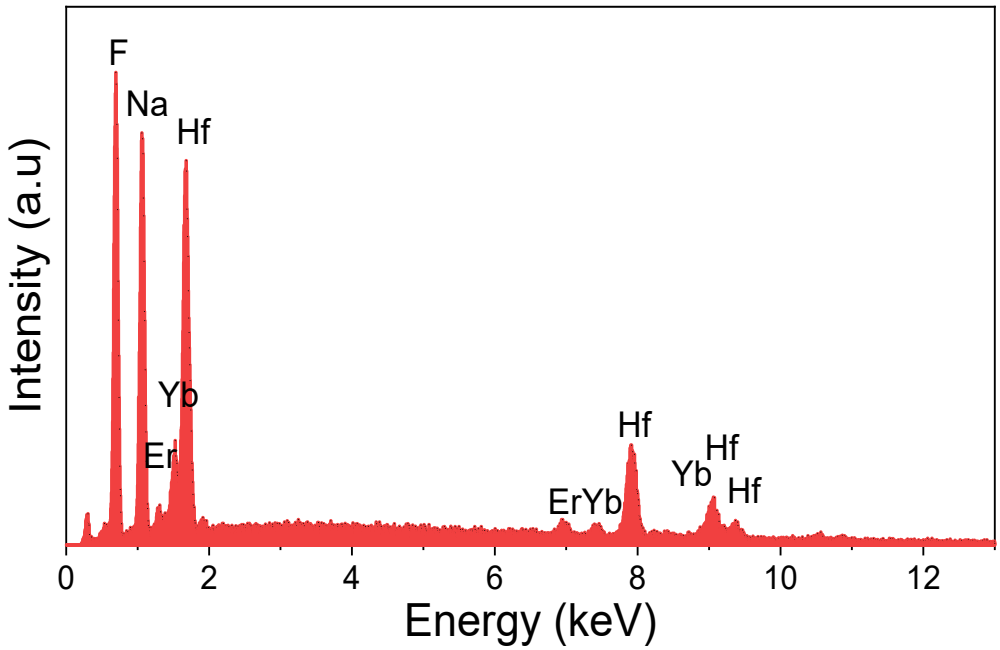

Figure S3. EDX spectrum of the Na_3HfF_7: 2Yb/6Er NPs.

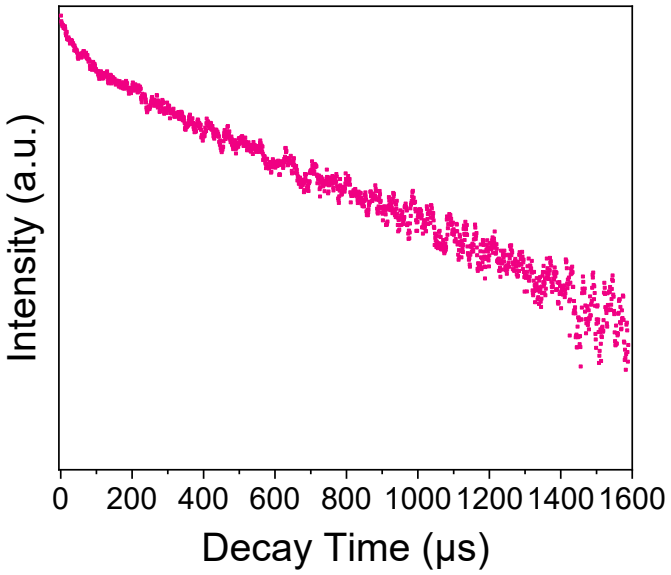

Figure S4. Decay curves of Er^{3+}: $^4F_{9/2} \rightarrow {}^4I_{15/2}$ in the Na_3HfF_7: 2Yb/6Er NPs.

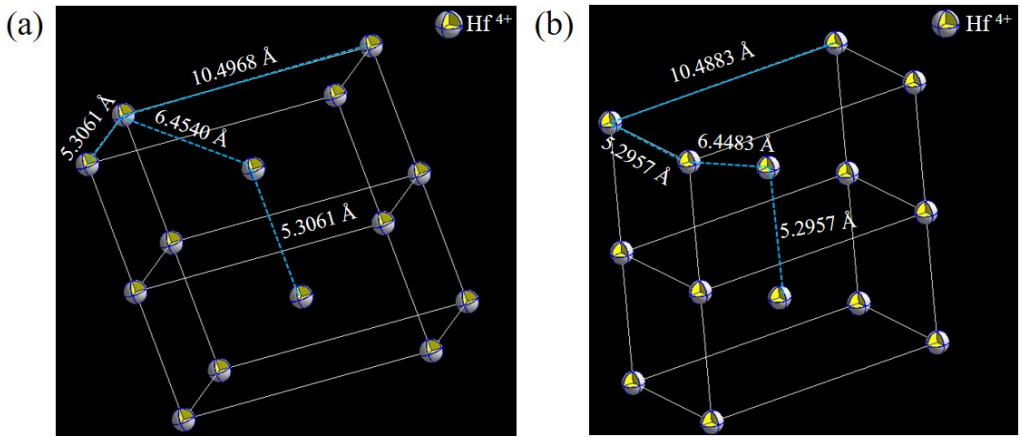

Figure S5. Schematic illustration of the Hf^{4+} lattice in the pure Na_3HfF_7 (a) and Na_3HfF_7: 2Yb/6Er NPs (b).

Considering the doped lanthanide ions are occupied in the Hf^{4+} lattice, the nearest Er – Er distance is calculated to be 5.2957 Å. The energy transfer efficiency between sensitizers and activators P_{SA}(dd) can be expressed by the equation of

$$P_{SA}(\mathrm{dd}) = \frac{1}{(2J_i+1)(2J_l+1)}\left(\frac{2}{3}\right)\left(\frac{2\pi}{\mathrm{h}}\right)\left(\frac{e^2}{R_{SA}^3}\right)^2 \chi_{dd} \times \left[\sum_{\lambda}\Omega_\lambda \left\langle J_i \left\| U^\lambda \right\| J_j \right\rangle^2 \sum_{\lambda}\Omega_\lambda \left\langle J_l \left\| U^\lambda \right\| J_k \right\rangle^2\right] \cdot S$$

where R_{SA} represents the distance between sensitizers and activators (detailed information can be found in the literatures of T. Hoshine, J. Appl. Plus., 1967, 6, 1203 and T. J. Pushing, Physical. Soc., 1973, 34, 1918.). In this occasion, with the decrease of crystal lattice from (a=b=5.3061 Å, c=10.4968 Å) to (a=b=5.2957 Å and c=10.4883

Å), the energy transfer efficiency between Er – Er pairs is evidently increased.

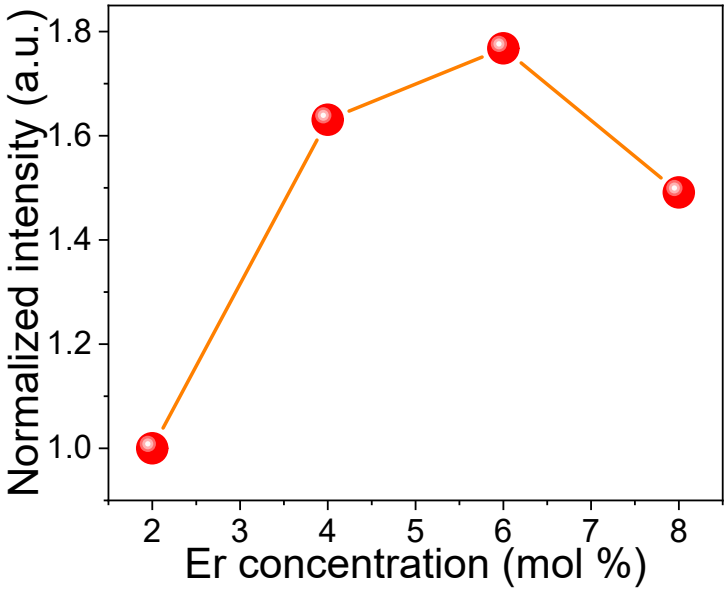

Figure S6. Initial afterglow intensity of the Na_3HfF_7: Yb/Er NPs doped with different Er^{3+} concentration.

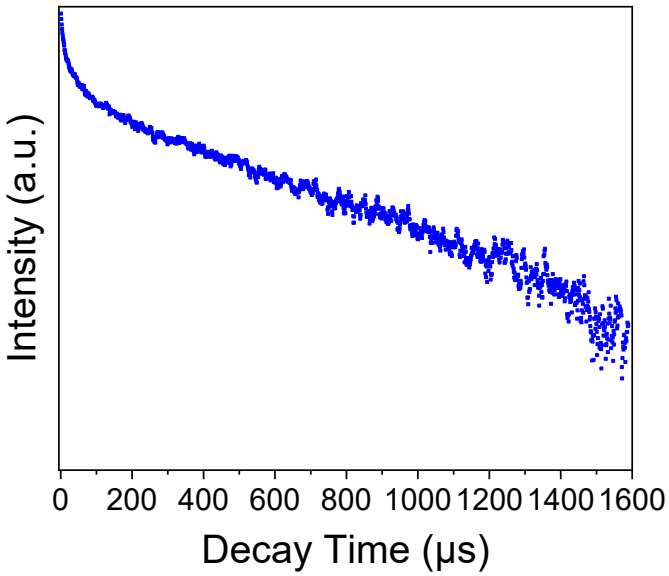

Figure S7. Decay curves of Tm^{3+}: $^3H_4 \rightarrow {}^3H_6$ in the Na_3HfF_7: 2Yb/0.5Tm NPs.

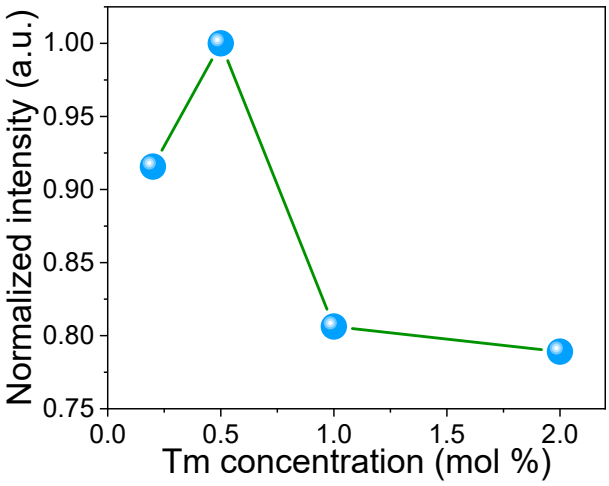

Figure S8. Initial afterglow intensity of the Na_3HfF_7: Yb/Tm NPs doped with different Tm^{3+} concentration.

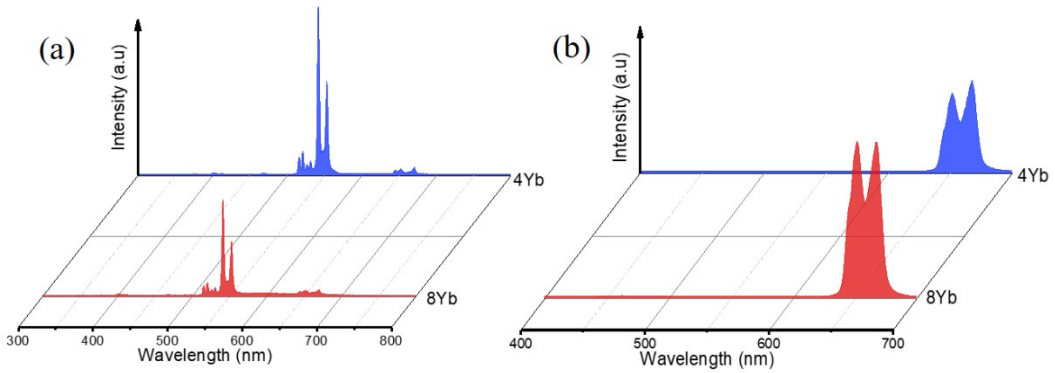

Figure S9. Scintillation (a) and UC (b) emission spectra of the Na_3HfF_7: Yb/6Er NPs doped with different Yb^{3+} ions concentration.

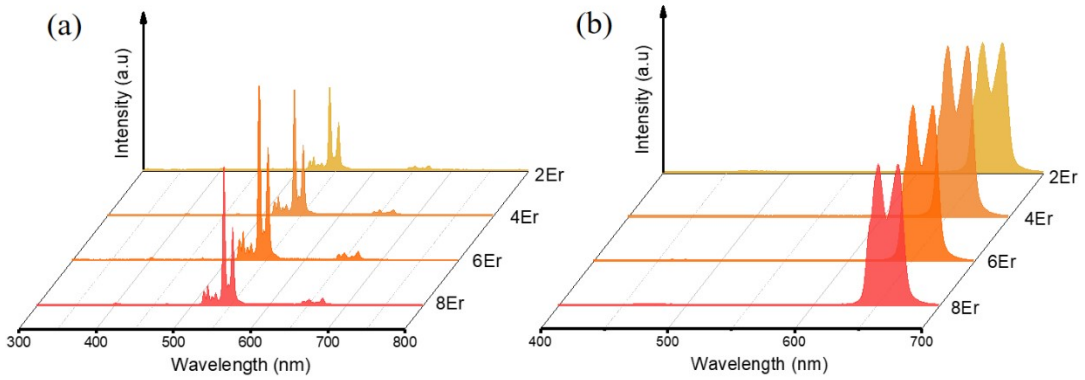

Figure S10. Scintillation (a) and UC (b) emission spectra of the Na_3HfF_7: 8Yb/Er NPs doped with different Er^{3+} ions concentration.

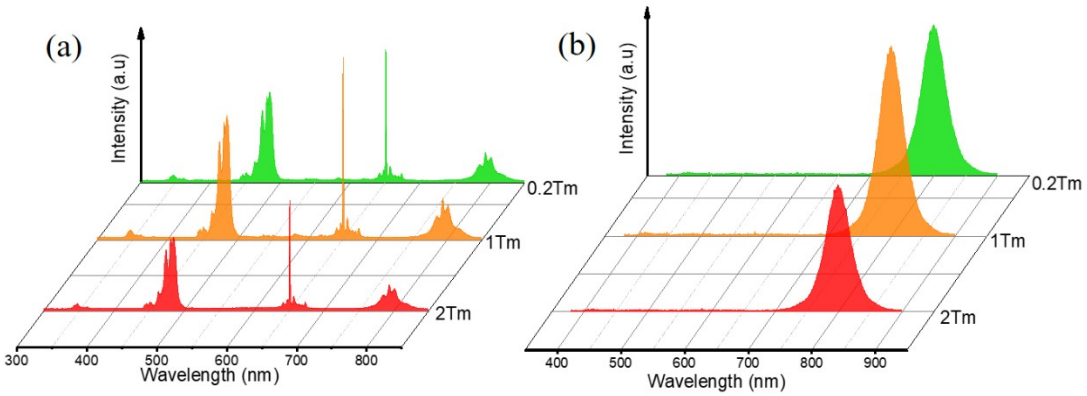

Figure S11. Scintillation (a) and UC (b) emission spectra of the Na_3HfF_7: 2Yb/Tm NPs doped with different Tm^{3+} ions concentration.

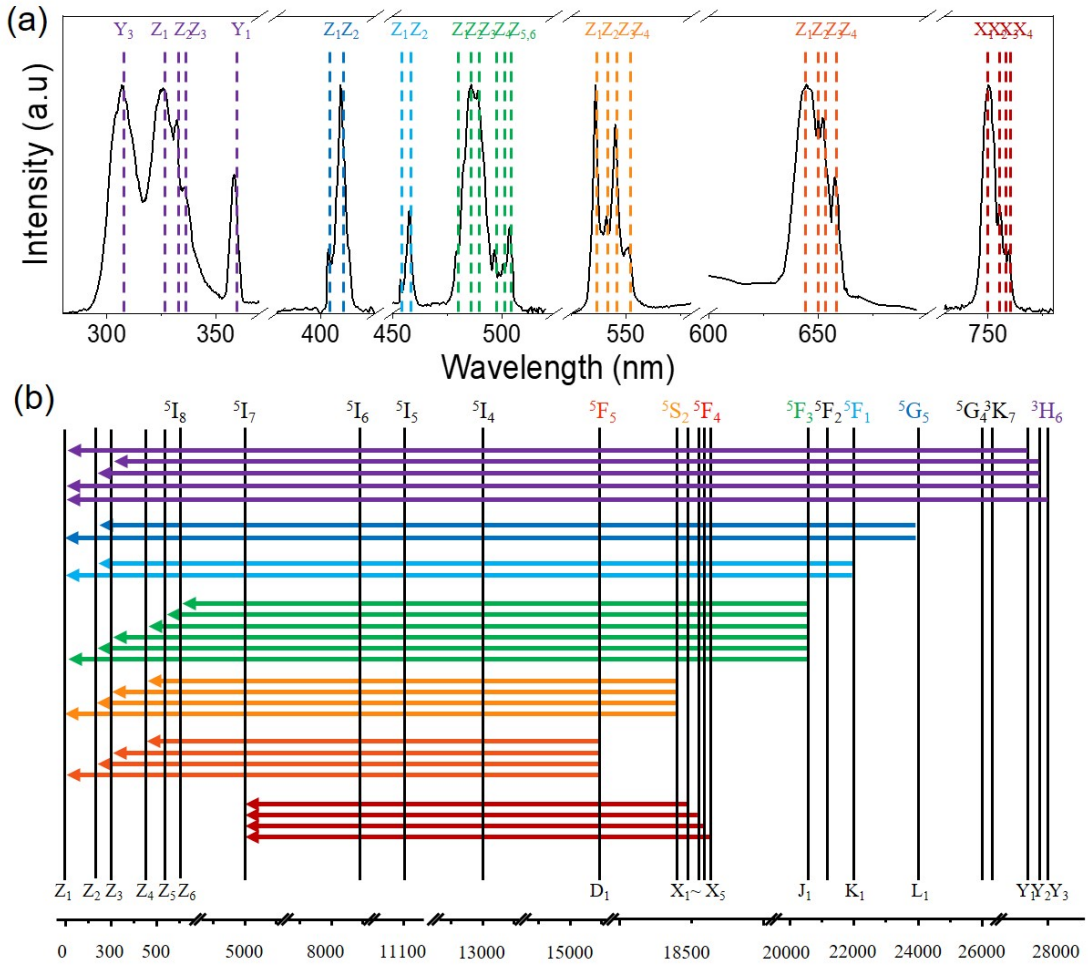

Figure S12. (a) Scintillation emission spectra of Na_3HfF_7: 2Yb/2Ho NPs. (b) Proposed crystal field energy levels of the Ho^{3+} in Na_3HfF_7 NPs, showing all crystal field transitions observed in (a).

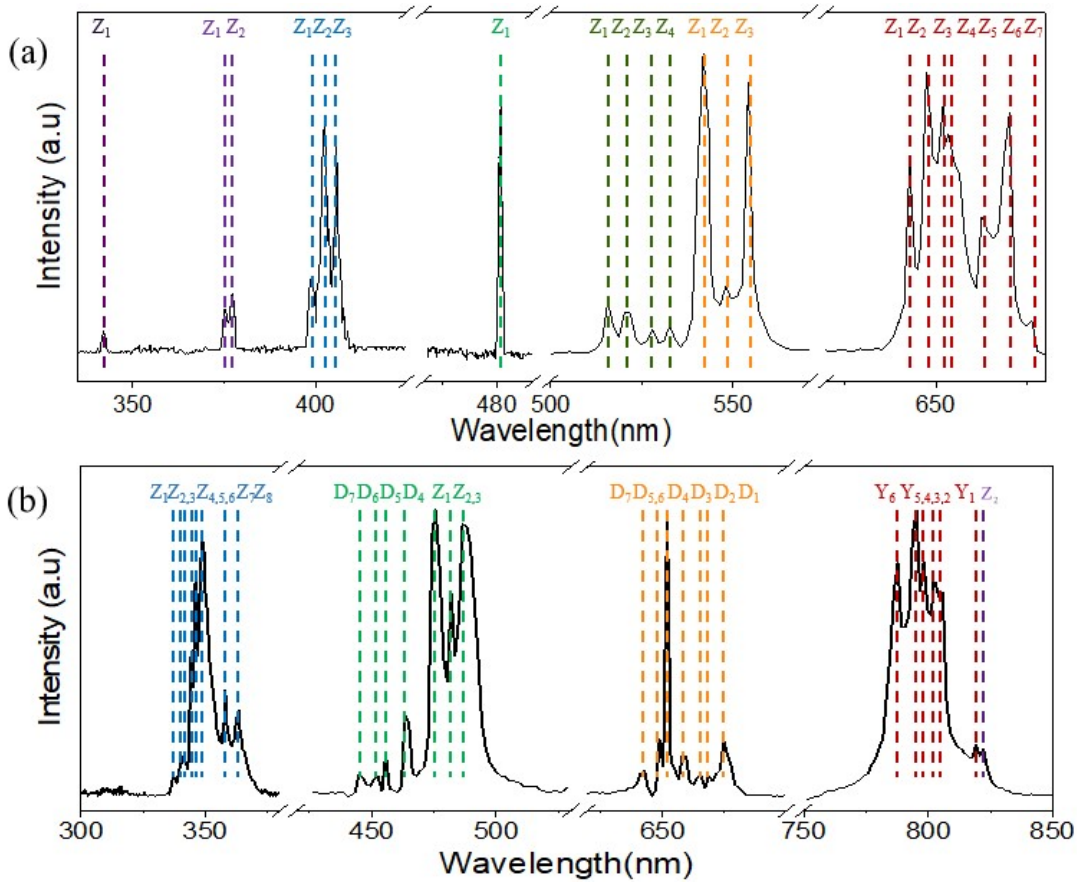

Figure S13. Scintillation emission spectra of the Na_3HfF_7: 2Yb/6Er NPs (a) and Na_3HfF_7: 2Yb/0.5Tm NPs (b) recorded at 77K. The Z_2 in the near infrared range corresponding to the transition of Tm^{3+}: Y_1 ($^3H_4$) → Z_2 ($^3H_6$).